Digest Journal of Nanomaterials and Biostructures Vol. 7, No. 3, July - September 2012, p. 1315 - 1325

PHYSICAL PROPERTIES EVALUATION OF ANNEALED $ZnAl_2O_4$ ALLOY THIN FILMS

R. CHANDRAMOHAN[a], V. DHANASEKARAN[b*], R. ARUMUGAM[c], K. SUNDARAM[d], J. THIRUMALAI[e], T. MAHALINGAM[b]
[a]*Department of Physics, Sree Sevugan Annamalai College, Devakottai – 630303, India.*
[b]*Department of Physics, Alagappa University, Karaikudi - 630 303, India*
[c]*Department of Physics, Government Arts College, Udumalpet – 642126, India*
[d]*Chendhuran College of Engineering & Technology, Pudukkottai – 622507*
[e]*Department of Materials Science & Engineering, Pohang University of Science and Technology (POSTECH), Gyeongbuk, 790-784, Republic of Korea*

Thin films of $ZnAl_2O_4$ were prepared by dip technique involving chemical solutions. Investigations on the effect of post heat treatment on the structural, optical and morphological properties of $ZnAl_2O_4$ thin films were studied. X-ray diffraction patterns revealed that the thin films are polycrystalline cubic structure of $ZnAl_2O_4$. The microstructural properties of $ZnAl_2O_4$ thin films were calculated and crystallite size tends to increase with increase of annealing temperatures. The texture coefficients have been evaluated and found to be greater than unity revealing high texturing of the architecture of the film. The transmittance spectra of unannealed and annealed films were plotted against UV-Vis-NIR region and found to be transmittance increases with annealing temperature. The optical band gap values were found to be in the range of 3.48 – 3.62 eV. The optical n and k constants were found to decrease with increase temperature of heat treatment. Scanning electron microscopic image revealed that the spherical shaped grains occupy the entire surface of the film and composition of the film was estimated using EDX spectra.

(Received June 20, 2012; Accepted September 4, 2012)

Keywords: Annealing; Alloys; Coatings; Microstructure

1. Introduction

Transition metal oxides possess a number of interesting optical and electrical properties. As thin films, they find applications in many electrical and optical devices. Zinc aluminate ($ZnAl_2O_4$) is a widely used ceramic, electronic and catalytic material with spinel structure [1]. $ZnAl_2O_4$ is also transparent to light with wavelengths above 320nm and is hence suitable for UV optoelectronic application and for use in thermal control coatings for spacecraft [2–4]. $ZnAl_2O_4$ is a well-known wide-bandgap semiconductor, an active component of catalysts, and also acts as a convenient support for other metal oxides and dispersed metals [5–7]. The preparation techniques for $ZnAl_2O_4$ thin films are many such as chemical vapor deposition (CVD) [8], hydrothermal [9], solid state reaction [10], spray pyroysis [11], microemulsions [12] and sol-gel spin-coating method [13]. However, all these techniques require sophisticated instruments and/or a high temperature of deposition. Among the thin films deposition methods, chemical bath deposition (CBD) from aqueous solutions is the simplest and most economical one [14]. The chemical bath deposition technique is simple, economical, and can be applied at room temperature. CBD method also offers the opportunity of doping the host ions with impurities on different kinds, shapes and sizes on substrates. The evaluation of optical dispersions and other optical constants of semiconductors are

* Corresponding author: v.j.dhanasekaran@gmail.com

of considerable importance for applications in integrated optic devices such as switches, filters and modulators, etc., where the refractive index of a material is the key parameter for device design.

It has good optical and catalytic properties. It has attracted interest as a phosphor host material for applications in thin film electroluminescent displays, mechano-optical stress sensors, and stress imaging devices. Green electroluminescence and stress-stimulated luminescence have been obtained in Mn-doped $ZnAl_2O_4$. Recently, a bright green cathodoluminescence (CL) under low excitation voltage from Mn-doped $ZnAl_2O_4$ thin films prepared by spray pyrolysis have been reported [11]. However, to our best knowledge, little research has been done on the cathodoluminescence of variety of rare-earth-doped $ZnAl_2O_4$ thin films. Moreover, the optical bandgap of polycrystalline $ZnAl_2O_4$ is 3.8 eV, indicating that $ZnAl_2O_4$ is transparent for light possessing wavelengths 320 nm. Therefore, it is widely used as a high-temperature material, ultraviolet photoelectronic material, optical and electronic coating, catalyst and catalyst support [15–17]. High surface area and accessible porosity are desirable properties in some applications of $ZnAl_2O_4$ films; for example, the catalytic properties of $ZnAl_2O_4$ films are largely dependent on their microstructure with a high surface area [18,19]. The wide band gap nature of the materials has been a limitation in producing devices for certain applications. Doping has been considered as one of the ways to alter the band gap [20]. Earlier using an aluminum foil, HF and zinc salts this interesting ceramic system has been reported by our group. [21-22]. In the present work, the chemical bath deposition using a double dip technique has been used for preparing $ZnAl_2O_4$ thin films and the effect of annealing properties on the physical properties of the films are discussed. The structural, morphological and optical properties of these films have been studied and the effect of annealing on these properties has been investigated. Different heating rates were chosen to study the effect of heating conditions on the microstructural development and the formation of surface topography of $ZnAl_2O_4$ films prepared by a soft chemical route which could be a cost effective and easy method. Possible mechanisms for microstructure development of $ZnAl_2O_4$ films are discussed.

2. Experimental

In this study $ZnAl_2O_4$thin films were prepared by extending the double dip technique [14] by varying deposition parameters such as solvent medium, solution pH, concentrations, temperature, number of dippings, etc., The effect of these parameters are studied using various characterizations and the optimized deposition parameters are arrived. The ‘Al ‘introduction was carried out by adding the aluminum salts in the solution bath at different proportions (Zn: Al $<$ 10 : 1). Before deposition, the glass substrates were cleaned by chromic acid followed by cleaning with acetone. The well-cleaned substrates were immersed in the chemical bath for a known standardized time followed by immersion in hot water for the same time for hydrogenation. The process of solution dip (step 1) followed by hot water dipping (step 2) is repeated for known number of times. The cleaned substrate was alternatively dipped for a predetermined period in sodium zincate (with Aluminum salt) bath and water bath kept at room temperature and near boiling point, respectively. According to the following equation, the complex layer deposited on the substrate during the dipping in sodium aluminum zincate bath will be decomposed to $ZnAl_2O_4$ due to dipping in hot water. The proposed reaction mechanism is according to the following equations [14]

$$Al_2(SO_4)_3 + ZnSO_4 + 2NaOH \rightarrow Na_2Al_2Zn(SO_4)_4(OH)_2$$
$$Na_2Al_2Zn(SO_4)_4(OH)_2 + 2H_2O \rightarrow ZnAl_2O_4 + 4H_2SO_4$$

Part of the so formed was deposited onto the substrate as a strongly adherent film and the remainder formed as a precipitate. The addition of aluminum sulphate in the ratio of Zn:Al as 10:1 in the first dip solution has been used in the formation of $ZnAl_2O_4$ films. For air annealing the samples a furnace is employed. The post annealing temperatures and time were selected by the stability of the samples.

The crystalline structure was determined by X-ray diffraction using X'PERT PRO (PANalytical) diffractometer with Cu K_α radiation (α = 0.15405 nm) and employing a scanning rate of 5°min^{-1}. The particle size and morphology was examined in a scanning electron microscope (SEM) Hitachi S-3000H model. For SEM studies the powders are pre-coated with Au sputtering using fine coat ion sputter JFC-1100 model instrument. Optical transmittance was measured by Perkin Elmer Lambda 35 UV-Vis spectrophotometer. All the measurements were performed at room temperature.

3. Results and discussion

Fig. 1 shows the X-ray diffraction patterns of $ZnAl_2O_4$ films with and without annealing temperature (a) as-deposited (b) 200^0C (c) 300^0C and 400^0C. The observed results are good agreement with standard "d-spacing" values (JCPDS diffraction file no. 65-3104) suggests that the material deposited is cubic $ZnAl_2O_4$ structure. Also X-ray diffraction patterns indicate that the various diffraction peaks at 2θ values 31.35, 34.13, 54.91 and 74.11, are identified to originate from (220), (002), (422) and (620) planes, respectively, which corresponds to $ZnAl_2O_4$ face centered cubic phase. The predominant peak at angle 2θ = 31.35^0 corresponds to the crystallographic plane (220) reflection for $ZnAl_2O_4$. Figure 1(a) XRD pattern revealed that the unannealed sample has lower intensity diffraction lines. The annealed films XRD patterns were produce a considerable improvement in crystallinity, showing more intense and sharper diffraction peaks. Also the number of diffraction lines is increased in $ZnAl_2O_4$ orientations with increase of annealing temperatures. XRD patterns predicted that when increasing the annealing temperature from 0 to 200^0C two new peaks emerged in the orientation of (422) and (620). Also all the peaks are highly intense it maximum annealing temperature it may be due to the increase crystallinity of the films. No typical peaks have appeared when increasing the annealing temperature above 200^oC. It is observed that the $ZnAl_2O_4$ are highly intense with good poly crystalline structure to improve the optoelectronic properties of the film. Similar findings were also reported by other authors [16,17].

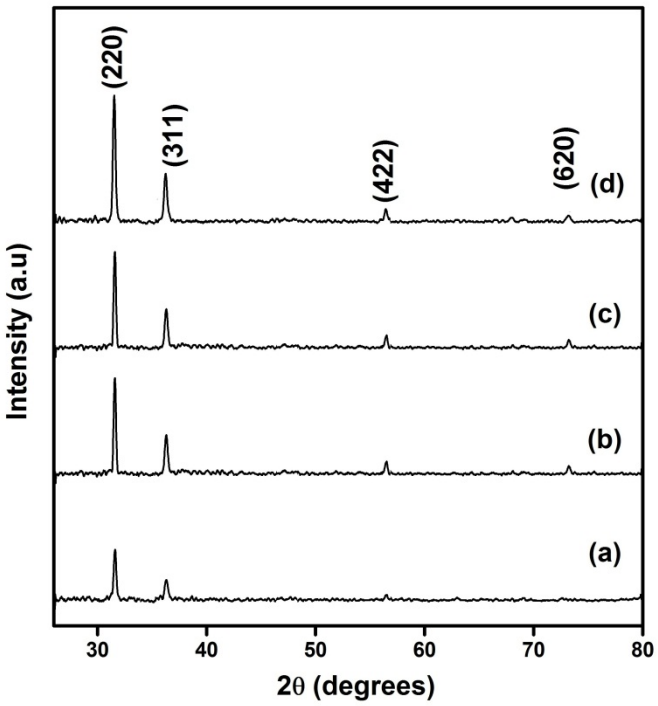

Fig. 1 X-ray diffraction patterns of $ZnAl_2O_4$ thin films (a) un annealed (b) 200^0C (c) 300^0C and (d) 400^0C

Fig. 2 shows that crystallite size of the $ZnAl_2O_4$ thin film with various annealing temperatures. The crystallite size D of the films was calculated from the Debye-Scherer's [18] formula D = [0.9λ/βcosθ],where D is crystallite size and β is the FWHM. The larger FWHM observed for all the XRD peaks show that the $ZnAl_2O_4$ films have nanocrystallites and the calculated crystallite size is of the order of 26.6 - 29.7 nm. The maximum broadening of peak is observed in unannealed condition. Crystallite size of the film increases with annealing temperature and is as shown in figure 2. The post heat treatment increases the crystallinity of the film. It also improves the crystallite size and its thermal expansion properties.

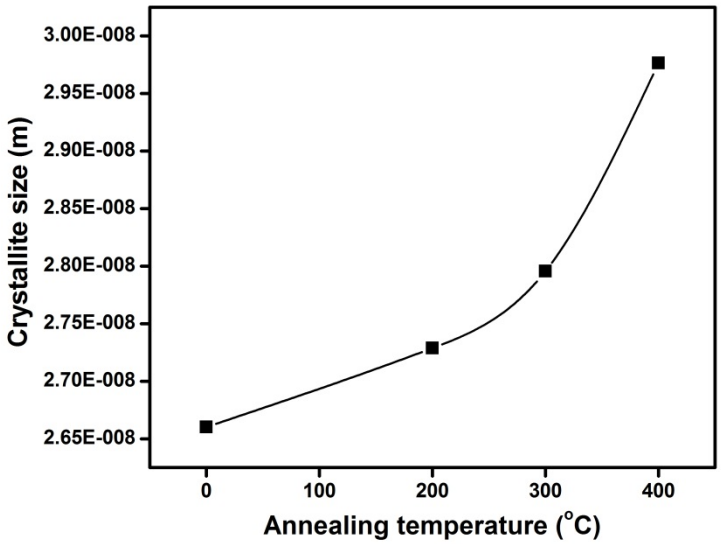

Fig. 2 Crystallite size and thickness of $ZnAl_2O_4$thin films with annealing temperatures

The calculated crystallite size of the film and their corresponding texture coefficient (*P*) is estimated. The texture coefficient was calculated using an expression

$$P(h_i k_i l_i) = \frac{I(h_i k_i l_i)}{I_0(h_i k_i l_i)} \left[\frac{1}{n} \Sigma \frac{I(h_i k_i l_i)}{I_0(h_i k_i l_i)} \right]^{-1} \quad (1)$$

where I_0 represents the standard intensity, I is the observed intensity of $(h_i k_i l_i)$ plane and n is the reflection number. The crystallite shape of the $ZnAl_2O_4$ film is strongly related to the texture coefficient of the film. The annealing effect of the texture coefficient values for different lattice plane $ZnAl_2O_4$ thin films are shown in figure 3. $P(h_i k_i l_i)$ has to be bigger that 1 to determine the preferential orientation [19], if $P(h_i k_i l_i)$ approximately 1 for all the $(h_i k_i l_i)$ planes considered at X-ray diffraction patterns, the films are randomly oriented $P(h_i k_i l_i)$values higher than one indicates the abundance of grains in a given $(h_i k_i l_i)$ direction and $0< P(h_i k_i l_i)<1$ values indicate the lack of grains oriented in that direction [20]. The predominant plane orientation of the film has high texture coefficient value. Generally, the texture coefficient value is maximum for its predominant orientation of the film and in this case predicted another one peak orientation also has more than 1 value of texture coefficient is as shown in figure with annealing temperature for predominant peak. It has been reported for copper oxide film [23] earlier that texture coefficient higher than 1 indicates preferential orientation and also indicates the abundance of grains in a given (h_i,k_i,l_i) direction.

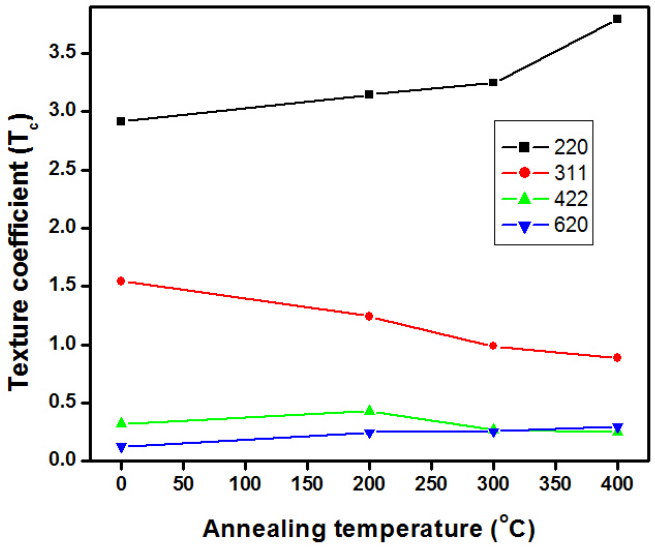

Fig. 3 Texture coefficient of $ZnAl_2O_4$thin films with annealing temperatures

The relation connecting stacking fault probability (α) with peak shift Δ(2θ) was given by

$$\alpha = \left(2\pi^2 \Big/ 45\sqrt{3} \right) \left[\Delta(2\theta) \Big/ \tan\theta \right] \tag{2}$$

where D is crystallite size, β is full width at half maximum, α stacking fault probability and λ wavelength of the X-ray diffraction. The number of crystallites per unit area (N) of the films was determined with the use of the following formula:

$$N = \frac{t}{D^3} \tag{3}$$

where t is thickness of the film and D is the crystallite size. Figure 4 shows that stacking fault probability and number of crystallites per unit area versus annealing temperatures. X-ray line profile analysis revealed that the crystallite size increases with annealing temperature and the films are found to have maximum value of crystallite size of 29.7 nm. So that the stacking fault probability of the film is decreased due to increase of crystallite size. It is also observed that the number of crystallites per unit area is found to decrease with annealing temperature. As the annealing temperature is increased, it is evident that the crystallite size increases and in turn the number of crystallites per unit area is decreased.

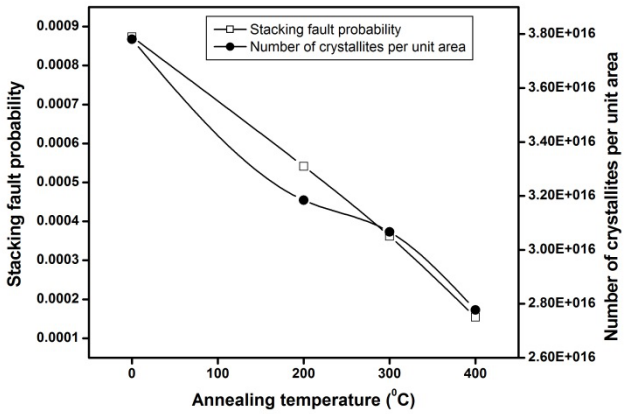

Fig. 4 Stacking fault probability and number of crystallites per unit area of $ZnAl_2O_4$ thin films

The strain ε was calculated from the slope of $\beta cos\theta$ versus $sin\theta$ [24]. Dislocation density of the films can be calculated using the below expression

$$\delta = n/D^2 \tag{4}$$

where D is the crystallite size. Figure 5 shows micro strain and dislocation density with various annealing temperatures. Also it is observed that the both of the microstructural properties are depend on the crystallite size of the film. So that microstrain and dislocation density of the films is decrease with increase annealing temperature. Due to the removal of defects in the lattice with increase in annealing temperature the microstrain in the films get released and attained a minimum value at 400^0C. A sharp increase in crystallite size and decrease in microstrain with annealing temperature is shown in figure 5. Such release in microstrain reduced the variation of interplanar spacing and thus leads to decrease in dislocation density and minimum values are obtained for films annealed 400^0C. A $ZnAl_2O_4$ thin film with lower microstrain, number of crystallites, stacking fault probability and dislocation density is improves the stoichiometry of the films which in turn causes the volumetric expansion of thin films.

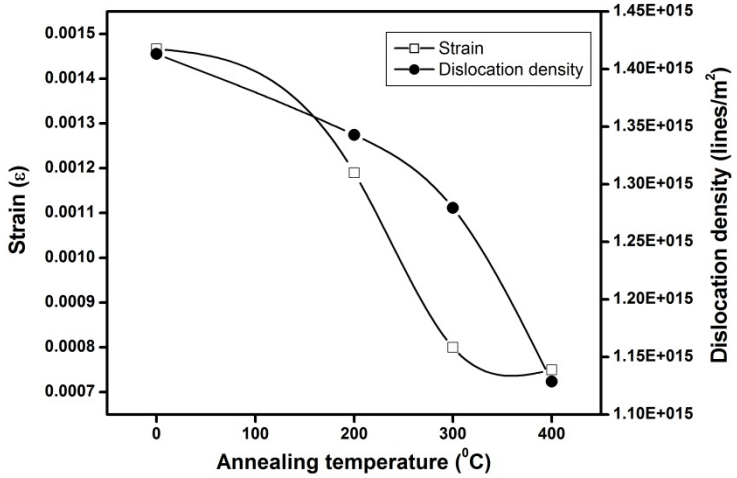

Fig.5 Strain and dislocation density of $ZnAl_2O_4$thin films with annealing temperatures

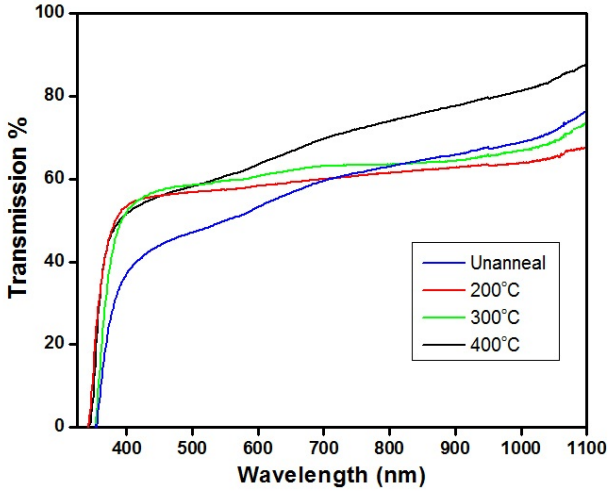

Fig. 6 Transmittance spectra of $ZnAl_2O_4$ thin films as function of wavelength

Figure 6 shows the transmittance of annealed and unannealed $ZnAl_2O_4$ films. The as-deposited film has 60% transmittance in the visible region and increase transmittance with annealing temperature up to 400°C. From this figure we have to conclude that as-deposited and 200°C annealed films have approximately the same transmittance property but above this annealing temperature the film emit maximum range of transmittance spectra. When the film is subjected to post heat treatment the optical properties are entirely increased. The increase in the transmittance is due to an increase in crystallite size of the film and it may affect the band gap of the film. The optical parameters such as absorption coefficient and band gap are determined from optical absorption measurements. The value of absorption coefficient for strong absorption region of thin film is calculated using the following equation (5) [26],

$$\alpha = \frac{1}{t}\ln\left(\frac{A}{T}\right) \tag{5}$$

where α is the absorption coefficient in cm^{-1}, t is the thickness of the films, A is absorbance and T is transmittance. The nature of transition is determined using the following equation (6) [25],

$$\alpha h\nu = A\left(h\nu - E_g\right)^n \tag{6}$$

where α is absorption coefficient in cm^{-1} , hν is photon energy, Eg is an energy gap, A is energy dependent constant and n is an integer depending on the nature of electronic transitions. For the direct allowed transitions, n has a value of 1/ 2 while for indirect allowed transitions, n = 2.

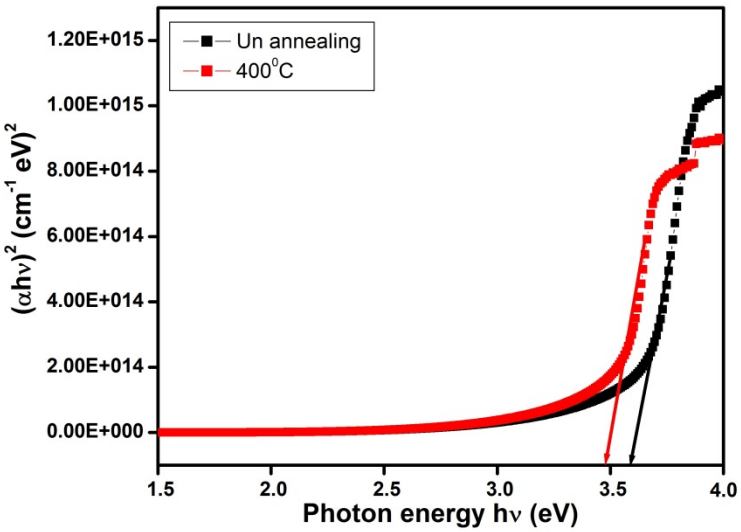

Fig. 7 Band gap variation of $ZnAl_2O_4$ thin films using conventional method

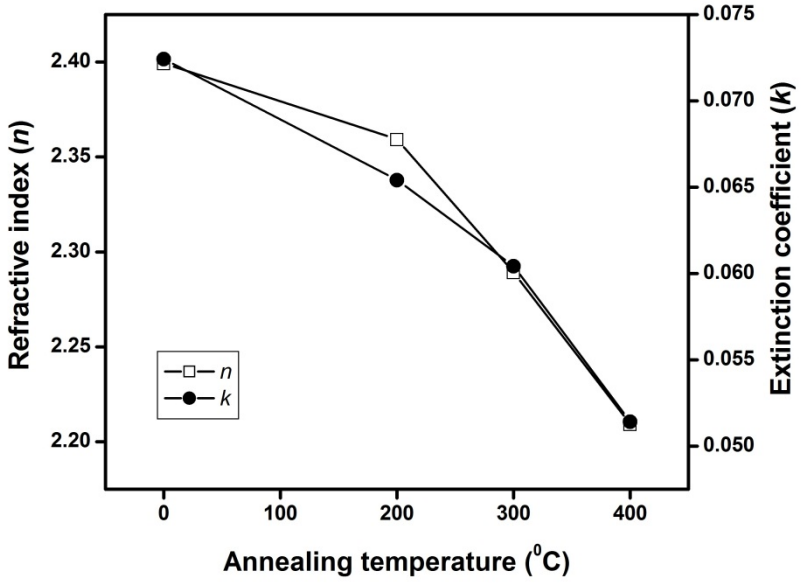

Fig. 8 Refractive index and extinction coefficient of $ZnAl_2O_4$ thin films versus various annealing temperatures

The band gap energy of the grown thin films can be determined by extrapolation of the linear part of the plot of $(\alpha hv)^2$ versus the incident radiation energy, hv as shown in figure 7; which indicates that the near band edge optical absorption coefficient has spectral dependence of only the joint density of states in samples. The optical absorption edge has been observed at a wavelength of about 355 nm corresponding to band gap energy of about 3.48 eV for un- annealed sample. The observed band gap energy of the annealed sample is about 3.62eV corresponding to a wavelength of 340 nm. These results show that the band gap energy of $ZnAl_2O_4$ thin film shifts to higher energy values after annealing. They attribute the optical absorption edge to increasing crystallinity of the $ZnAl_2O_4$ alloy films. However, the band gap can be changed by the alterations in the oxygen sites. The increase in the band gap may be associated with decrease in oxygen content in the film

that might have been caused due to the annealing. As temperature of annealing is increased more oxygen is absorbed in the process that could cause a decrease in the oxygen content in the films.
We have further investigated the experimental data of optical transmittance and reflectance of $ZnAl_2O_4$ thin film to calculate the refractive index and the extinction coefficient. Optical transmission and reflection spectra were recorded at room temperature in air to obtain information on the optical properties of $ZnAl_2O_4$ thin films. Refractive index (n) and extinction coefficient (k) of $ZnAl_2O_4$ films are estimate using the expressions [26],

$$n = \frac{1+R}{1-R} + \sqrt{\frac{4R}{(1-R)^2} - k^2} \tag{7}$$

$$k = \frac{\alpha\lambda}{4\pi} \tag{8}$$

where α is absorption coefficient, λ is wave length of the $ZnAl_2O_4$ alloy thin films. The refractive index and extinction coefficient of the films are decreased when increasing the annealing temperature shown in figure 8. The refractive index of the films increased rapidly with the increase of annealing temperature also extinction coefficient values. The initial sharp increase of 'n' with 'k' indicated a rapid change in the absorption energy of the unannealed films. Generally the refractive index of ZnO thin film was decreased at longer wavelength regime and also it is found to decrease after Al incorporation in ZnO matrix.

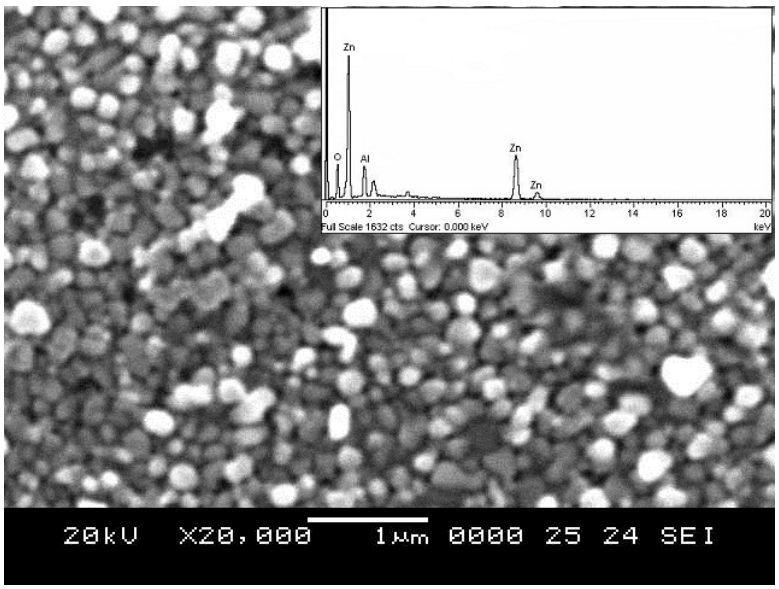

Fig. 9 SEM picture of $ZnAl_2O_4$thin film annealed at 400^0C and inset figure shows EDX spectrum

Figure 9 shows the SEM picture of $ZnAl_2O_4$ chemical bath deposited annealed at 400^0C. The annealed (400^0C) film there is an increase in crystallite size. The surface morphology of $ZnAl_2O_4$ film annealed at 400^oC is characterized by a number of compact bright contrast spots in nano scale, as shown in Fig. 9. This result in an increase in nucleation over-growth and the deposits are more compact with uniform grain structure. An increase in the size of the crystallites with anneal temperature was also evident from the SEM picture. It is observed from scanning electron micrographs that the average grain sizes of $ZnAl_2O_4$ films annealed at 400^0C is 100nm. Fig.9 revealed that grains become larger and more uniform as the film was annealed at 400^0C. The composition of the 400^0C annealed $ZnAl_2O_4$ thin film is obtained using EDX spectrum shown in inset fig. 9. The EDX spectrum has revealed that the oxygen content slightly decrease annealed at 400^0C.

4. Conclusions

The optical and structural characterization of as deposited and annealed samples have shown that the thermal treatment carried out at 200^0C, 300^0 C and 400^0C has a great influence on the physical parameters of the grown structures. The XRD results reveal that the deposited thin film has a good polycrystalline cubic structure. The films without annealing have the crystallite size lower than those films annealed at temperatures of 200^0C, 300^0C and 400^0C. The microstructural parameters were estimated and were found to depend on the post heat treatment the $ZnAl_2O_4$ thin films. The optical transmittance has increases from 50 % to 80% in visible region with increase of annealing temperatures. It has been observed that the direct band gap energy was increased from 3.48 to 3.61 eV after annealing from 0 to 400^0C for 60 min under air medium. We propose that this increase in band gap energy may be due to the low oxygen content of the sample surface after thermal treatment. The refractive index and extinction coefficient showed some variation with rise in annealing temperature of $ZnAl_2O_4$ thin film. The surface morphology of $ZnAl_2O_4$ film annealed at 400^oC is revealed by a number of compact bright contrast spots in nano scale region. The annealing effects on the structural and optical properties of $ZnAl_2O_4$ thin film on glass substrate will be useful for the formation of $ZnAl_2O_4$ based polycrystalline films for the application of optoelectronic devices.

Acknowledgment:

We dedicate this paper to Dr. R. Arumugam one of the co-author who has passed away recently in an unexpected road accident.

References

[1] R. Pandey, J.D. Gale, S.K. Sampath, J.M. Recio, J. Am. Ceram. Soc. **82**, 1337 (1999).
[2] S.K. Sampath, J.F. Cordaro, J. Am. Ceram. Soc. **81**, 649 (1998).
[3] A.E. Galetti, M.F. Gomez, L.A. Arrúa, M.C. Abello, Appl. Catal. A: Gen. **348**, 94 (2008).
[4] L.M. Chen, X.M. Sun, Y.N. Liu, K.B. Zhou, Y.D. Li, J. Alloys Compd. **376**, 257 (2004).
[5] K.E. Sickfaus, J.M. Wills, J. Am. Ceram. Soc. **82**, 3279 (1998).
[6] M.C. Marion, E. Garbowski, M. Primet, J. Chem. Soc., Faraday Trans. **87**, 1795 (1991).
[7] C.O. Arean, B.S. Sintes, G.T. Palomino, C.M. Carbonell, E.E. Platero, J.B.P. Soto, Microporous Mater. **8**, 187 (1997).
[8] G. Fang, D. Li, B.-L. Yao, J. Crystal growth **247**, 393 (2003).
[9] Z. Chen, E. Shi, Y. Zheng, W. Li, N. Wu, W. Zhong, Mater. Lett. **56**, 601 (2002).
[10] C.O. Arean, B.S. Sintes, G.T. Palomino, C.M. Carbonell, E. Scalona Platero, J.B. Parra Soto, Microporous Mater. **8**, 187 (1997).
[11] Z. Lou, J. Hao, Appl. Phys. A: Mater. Sci. Process. **80**, 151 (2005).
[12] A.E. Giannakas, T.C. Vaimakis, A.K. Ladavos, P.N. Trikalitis, P.J. Pomonis, J. Colloid Interface Sci. **259**, 244 (2003).
[13] S. Mathur, M. Veith, M. Haas, Haoshen, N. Lecerj, V. Huch, J. Am. Ceram. Soc. **84**, 192 (2001).
[14] T. A. Vijayan, R. Chandramohan, S. Valanarasu, J. Thirumalai, S. Venkateswaran, T. Mahalingam and S. R. Srikumar. Sci. Technol. Adv. Mater. **9**, 035007 (2008)
[15] N. Guilhaume, M. Primet, J. Chem. Soc., Faraday Trans. **90**, 1541 (1994).
[16] W.S. Tzing, W.H. Tuan, J. Mater. Sci. Lett. **15**, 1395 (1996).
[17] S.K. Sampath, J.F. Cordaro, J. Am. Ceram. Soc. **81**, 649 (1998).
[18] T. El-Nabarawy, A.A. Attia, M.N. Alaya, Mater. Lett. **24**, 319 (1995).
[19] M. Zawadzki, J. Wrzyszcz, Mater. Res. Bull. 35, 109 (2000).
[20] R. Romero, D. Leinen, E.A. Dalchiele, J.R. Ramos-Barrado, F. Martin, Thin Solid Films **515**, 1942 (2006).
[21] K. Kumar, K. Ramamoorthy, R. Chandramohan, and K. Sankaranarayanan, Journal of Nanoparticle Research **9**, 331 (2007).

[22] K. Kumar, K. Ramamoorthy, R. Chandramohan, and K. Sankaranarayanan, J. Cryst. Growth **289**, 405 (2006).
[23] S. Kose, F. Atay, V. Bilgin, I Akyuz Mater. Chem. Phys. 111,351 (2008).
[24] V.M. Nikale, N.S. Gaikwad, K.Y. Rajpure, C.H. Bhosale, K.M. Garadhar, Mater. Chem. Phys. **80**, 102 (2003).
[25] S Gopal, C. Viswanathan, B. Karunagaran, Sa. K. Narayandass, D. Mangalaraj J. Yi, Cryst. Res. Technol., 40(6), 557 (2005).
[26] T. Mahalingam, V. Dhanasekaran, G. Ravi, Soonil Lee, J. P. Chu, Han-Jo Lim J. Optoelectron. Adv. Mater. **12**, 1327 (2010).